Novel distributed passive vehicle tracking technology using phase sensitive optical time domain reflectometer

Zhaoyong Wang (王照勇)[1,2], Zhengqing Pan (潘政清)[1], Qing Ye (叶 青)[1,], Bin Lu (卢 斌)[1,2], Zujie Fang (方祖捷)[1], Haiwen Cai (蔡海文)[1,3,4,*], and Ronghui Qu (瞿荣辉)[1]**

[1]*Shanghai Key Laboratory of All Solid-state Laser and Applied Techniques, Shanghai Institute of Optics and Fine Mechanics, Chinese Academy of Sciences, Shanghai 201800, China*

[2]*University of Chinese Academy of Sciences, Beijing 100049, China*

[3]*Shanghai Synet Optics Technology Corporation, Shanghai 200135, China*

[4]*Bandweaver Technologies Co. Ltd., Shanghai 201203, China*

**Corresponding author: hwcai@siom.ac.cn; **corresponding author: yeqing@siom.ac.cn*

Received May 25, 2015; accepted July 31, 2015; posted online August 31, 2015

A novel distributed passive vehicle tracking technology is proposed and demonstrated. This technology is based on a phase-sensitive optical time domain reflectometer (Φ-OTDR) that can sense and locate vibrations. Two algorithms, dynamic frequency-space image and 2D digital sliding filtering, are proposed to distinguish a car's moving signals from severe environmental noises and disturbances. This technology is proved effective by field experiments for tracking a single car and multiple cars. This work provides a new distributed passive way for real-time vehicle tracking and this technology will be extremely important for traffic controlling and public safety in modern society.

OCIS codes: 060.2370, 230.0250, 290.5870.
doi: 10.3788/COL201513.100603.

Real-time vehicle positioning and tracking are very important in traffic control and public safety for some special locations such as residential regions, schools, and those areas near stadiums or exhibitions. Although some developed technologies, especially the Global Position System (GPS)[1], can track vehicles, their applications for this purpose are limited by concerns of privacy protection, additional terminal equipment for vehicles, expensive cost, and so on. The radio frequency (RF) identification[2,3] is widely used in logistics and the internet of things (IOT), but vehicles could only be detected in separate areas according to the separate RF receivers. Reference [4] proposed a method that laid RF receivers along roads and equipped testing vehicles with microprocessor transmitters. It is effective but the reliability is still a problem since the transmitter may fail to work due to some intentional or unintentional reasons.

A phase-sensitive optical time domain reflectometer (Φ-OTDR) has the capability of detecting dynamic disturbances along the fiber with the advantages of distributed sensing and almost all of the advantages of fiber vibration sensors[5–9] such as low cost, anti-electromagnetic interference, anti-corrosion, and so on. Vibrations and sounds from the vehicle's movement cause the sensing fiber to vibrate and the scattering light phase to change accordingly. As a dynamic sensor, Φ-OTDR can detect the vibration in real time, demodulate the phase variation, and obtain its spatial position along the fiber. So this technology is quite suitable for intrusion alarming and vehicle tracking.

Reference [10] described an Φ-OTDR technology for locating and speed monitoring of trains that run on the railway at high speed. For tracking a vehicle on the ground, the traffic situation and environment are much more complex than those of the railway and a weak vehicle tracking signal is usually buried under a higher environmental disturbance level. Some new algorithms for noise suppression will be very important. In this Letter, we proposed and demonstrated a novel vehicle tracking technology by using a Φ-OTDR that can sense vibrations and locate their positions. Two algorithms, dynamic frequency-space image and 2D digital sliding filtering, are proposed to distinguish a car's moving signals from severe environmental noises and disturbances. The research results show that this technology is effective and accurate in tracking a single car and multiple cars. This work can provide a new distributed passive way for real-time vehicle tracking. We believe that this technology will be extremely important for traffic controlling and public safety in modern society.

The phase-sensitive OTDR in experiments is similar to that used in Ref. [11], as illustrated in Fig. 1(a). The system is composed of a distributed feedback fiber laser (DFB-FL) with a 5 kHz linewidth, an 160 MHz frequency-shift acousto-optic modulator (AOM) to chop the laser beam into pulses with a 200 Hz repetition rate and 50 ns pulse width, an erbium-doped fiber amplifier (EDFA) for amplifying the probe optical power, a double balanced photodetector (DB-PD) for coherent detection[12] to detect the beat signal of the returned wave and local oscillation, and a data acquisition card (DAQ) with a

 © 2015 Chinese Optics Letters

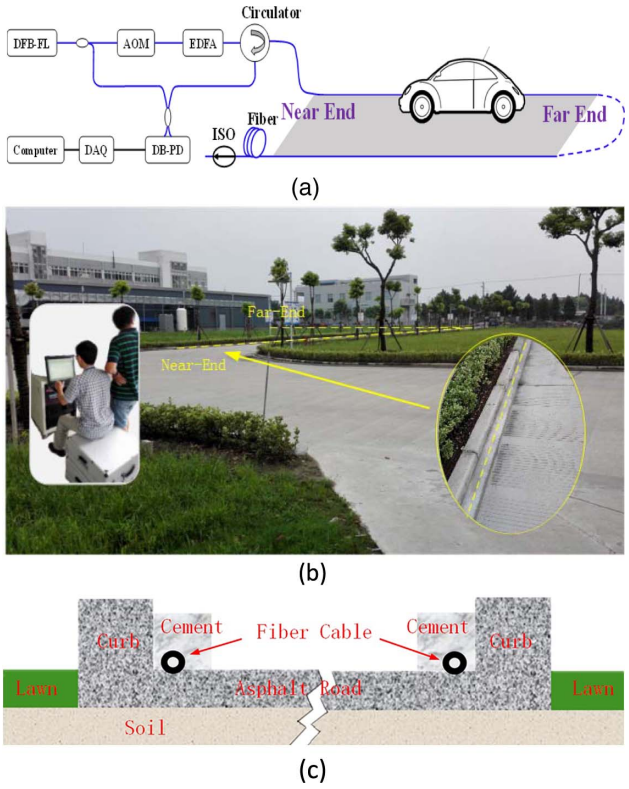

Fig. 1. (a) Experimental setup of Φ-OTDR; (b) photo of the experimental field; (c) installation structure of the sensing cable and the road (road cross section).

500 MHz sampling frequency. The beat signal is a function of the optical phase, which is related to the refractive index variation along the sensing fiber. The complex composite scattering Rayleigh coefficient $\tilde{r}_c(z)$ at position z is expressed as[9]

$$\tilde{r}_c(z) = \int_z^{z+\Delta z} \mathrm{d}x \cdot r_{\mathrm{Ray}} \exp[j2k \int_z^x \Delta n(y)\mathrm{d}y] = r_c e^{j\phi_c}, \quad (1)$$

where Δz is the fiber length corresponding to the probe pulse width. r_{Ray} is the composite Rayleigh scattering coefficient within the data acquisition period; k is the phase constant; $\Delta n(y)$ is the refractive index variation against position y, and y is an integral variable from z to x; x is an integral variable from z to $z+\Delta z$;r_c is the amplitude, and ϕ_c is the phase of $r_c(z)$. The beat signal I_{beat} can be given by[11]

$$I_{\mathrm{beat}} = |E_L|^2 + |r_c E_P|^2 + 2|r_c E_P E_L| \sin(\Delta\omega t + \phi_c), \quad (2)$$

where E_L and E_P are the fields of local oscillation and the probe, respectively, and $\Delta\omega$ is the frequency shift of AOM. The backward signal amplitude E_{Back} can be given as[11]

$$E_{\mathrm{Back}} = r_c E_P \propto \mathrm{abs}\left(\int_{t-\Delta T/2}^{t+\Delta T/2} AC \times \exp(i\Delta\varpi t')\mathrm{d}t'\right), \quad (3)$$

where AC represents the alternating part of the beat signal and ΔT is the range of integration, which determines the spatial resolution. The polarization state is neglected for simplicity.

The sensing cable in the experiment is an ordinary two-fiber nonarmored cable. The cable is buried on two sides of the road, as illustrated in Fig. 1(c). The cross section of the road was shown. The fiber cable was first fastened by a normal hasp near the curb on the pavement and then covered with cement to make the cable contact with the pavement tightly. Therefore, the vehicle's movement could vibrate the sensing cable effectively. Note that the sensitivity would increase greatly if the cable was buried when paving the road. In the photo of Fig. 1(b), the fiber cable was shown as the yellow dotted lines. The left side section is from the 10th meter (near-end) through the 210th meter (far-end), and the right one is from the 220th meter (far-end) through 430th meter (near-end). An optical isolator is used in the end of the sensing fiber to suppress the facet reflection.

An ordinary four-wheel car was used in the experiments. Figure 2 gives an example of the detected Φ-OTDR waterfall patterns when the car ran forward and then turned back from the near end to the far end of the road as far as 200 m. The colors stand for the demodulated amplitudes E_{Back} (Eq. (1) in Ref. [11]) of the beat signals. The signal seems to be hard to distinguish, but the trace of the car's movement can be indistinctly recognized as marked by the red elliptical lines in Fig. 2. The large noises are probably attributed to many environmental disturbances, for example, machine vibrations in nearby factories and buildings, trucks and cars running on nearby roads, and noises from some nearby construction sites. All of those noises must be reduced for practical applications. We use two methods for noise suppression, as follows.

The beat signal shown in Fig. 2 is the total beat intensity. It is suspected that there should be some differences in frequency spectra between vehicle's vibration and environmental noise. The Φ-OTDR is able to provide spectral information of the vibration due to its instantaneity. We processed the detected data by FFT and analyzed them by an algorithm termed the dynamic frequency-space image (DFSI). The DFSI gives out the frequency spectrum in a short period, step by step, sliding with the evolution

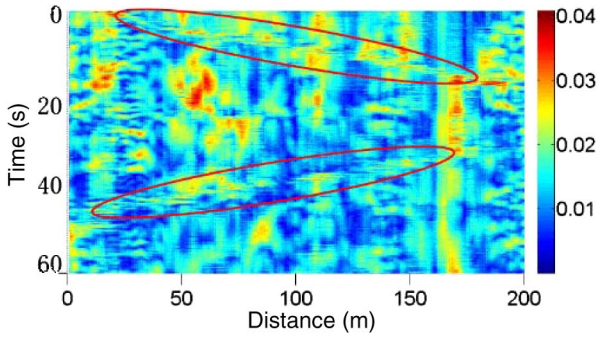

Fig. 2. Original waterfall pattern.

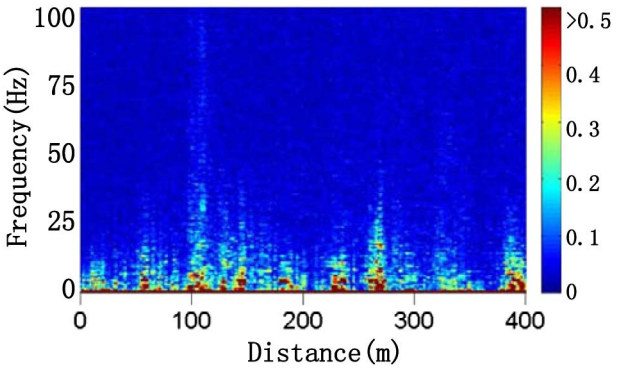

Fig. 3. DFSI pattern at the moment of the 10th second.

of time and distance. The sliding overlapping between neighboring steps is optional. Figure 3 gives a DFSI pattern at the moment of the 10th second, when a running car was located at the 110th meter from the starting point of the sensing fiber. Colors in DFSI stand for the intensity of spectrum, showing frequency spectra along the fiber. Figure 4(a) shows the frequency spectra at a position of the 110th meter; Fig. 4(b) is for a position of the 190th meter, 80 m away from the running car. It is seen that quite a high amplitude appears in the frequency band below 30 Hz, whereas the frequency of running-car-induced vibration is expanded up to 100 Hz.

Such spectral features are utilized in data processing by integrating the frequency component in the high frequency bands. Figure 5 shows the processed data for different integration frequency ranges. To compare the efficiency of different frequency integration range, the fluctuation ratio (FR) was proposed and defined as

$$\mathrm{FR} = (\text{signal-ground noise})/\text{the fluctuation of noise}. \quad (4)$$

Signals, ground noise, the fluctuation of noise, and the FR are shown in different colors in Fig. 5(g). Signal and noise both decrease with the increase of the low integration limit. The FR also changes and reaches the best value (about 3) with an integration range of 50–100 Hz.

As a comparison, Fig. 5(f) gives the original detected intensity at the same moment before DFSI processing, showing a notable improvement of the SNR. As the signal was submerged in the ground noise, the original FR cannot be calculated and it was supposed as zero for simplicity.

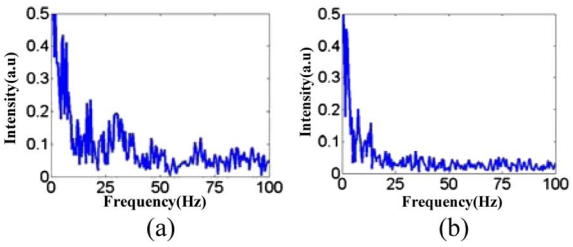

Fig. 4. Short period frequency spectra at positions (a) with and (b) without cars running.

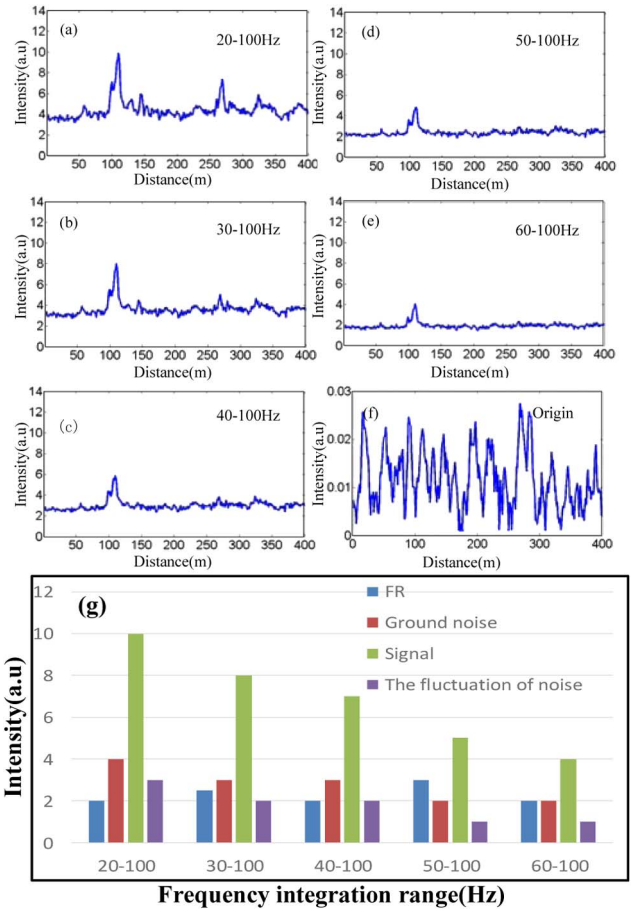

Fig. 5. DFSI processed signal, integrated over (a) 20–100, (b) 30–100, (c) 40–100, (d) 50–100, and (e) 60–100 Hz, compared with the original detected signal (f); (g) signals, ground noise, the fluctuation of noise and FR for frequency integration ranges above.

Figure 6 is the DFSI processed waterfall pattern for the difference between the signal and ground noise. The trace of the running car becomes clearly visible. Compared with the original waterfall of Fig. 2, a great improvement is achieved. The maximum difference between the signal and ground noise is 6 and the noise fluctuation could be estimated as about 2. As mentioned, the FR increased from zero to three. The car's velocity can be calculated from the figure, i.e., about 9.3 and 11.5 m/s for forward

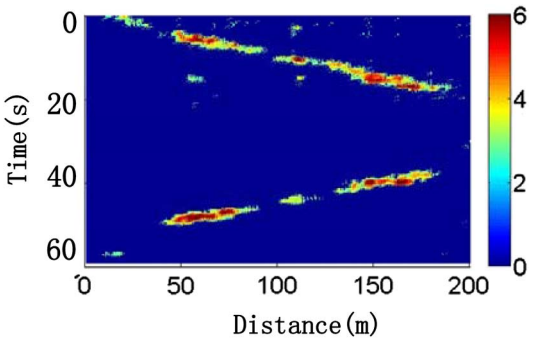

Fig. 6. DFSI processed waterfall pattern.

and backward running, respectively. It is noticed that some discontinuities appear in the traces. By checking on the spot we found that the discontinuities are mainly attributed to the laying defects of the sensing fiber where the fiber does not tightly contact the pavement, resulting in low sensitivity. Another possible factor is interference fading, which inevitably exists in the fiber.

After the DFSI processing the track is clearly obtained, but there is still some noise in the waterfall, as shown in Fig. 6. As observed in field experiments, the noise appears as isolated islands in the waterfall plot. To remove such noises, a 2D digital sliding filtering process is taken further that is similar to the neighbor average filtering in Ref. [13]. This algorithm integrates data in the neighbor of each data point including itself in the time-distance area. If the integrated result is less than the preset threshold, the data point will be set to zero. Every point must be dealt with in the waterfall figure and the process can be expressed as

$$S(i,j) = \sum_{x=i-L}^{i+L} \sum_{y=j-L}^{j+L} data(x,y), \tag{5}$$

$$data(i,j) = \begin{cases} 0, S(i,j) & < S_{\text{th}}, \\ data(i,j), & \text{others}, \end{cases} \tag{6}$$

where $data$ is the waterfall data being processed, $S(i,j)$ is the result integrated within a square of $(2L+1)\times(2L+1)$, and S_{th} is the preset threshold. The integral size and threshold should be selected carefully to get a good effect. Figure 7 gives the 2D digital sliding filtering processed result of the waterfall in Fig. 6, showing that the stray spots are removed thoroughly while the detected car traces are remained perfectly. As the fluctuation of noise was remarkably suppressed from 2 to less than 1, the FR was enhanced to more than 6.

FRs are listed in Table 1. The efficiency of the DFSI and 2D digital sliding filtering could be gotten clearly. A remarkable FR growth could be seen after using these two processing algorithms.

In practice, often several cars must be detected at the same time. Experiments for such situations were carried out. Figure 8 shows the waterfall pattern detected for four cars running one after another from the far end of the sensing fiber to the near end. The data have been processed by a DFSI and 2D digital sliding filtering.

Table 1. FRs in Different Processing Situations

	Original Waterfall	After DFSI	After DFSI & 2D Digital Sliding Filtering
FR	0	3	>6

In practical applications, real-time vehicle tracking is an extremely complex process and further work will be needed. Although the data processing algorithms have been proved effective in this Letter, it is still necessary to develop suitable algorithms for more complex application situations. More experiments with different vehicles under different environmental conditions should be carried out to acquire their detailed spectral characteristics and to extract features of moving vehicles in different situations.

Such information is the basis of distinguishing vehicle movement from environment noises and disturbances in various complicated situations. Meanwhile, the method of laying and burying sensing fibers should be optimized to improve their sensitivity and uniformity. In addition, some software problems should be considered, such as how to show cars on the map clearly when many cars are crossing on the same road. The related work is being undertaken by our group.

In conclusion, an approach of distributed passive vehicle tracking in monitored areas by Φ-OTDR is proposed in this Letter and the field experimental results are presented. To overcome the difficulties of severe environmental noise, two algorithms, DFSI and 2D digital sliding filtering, are proposed and demonstrated to process the detected beat signals, showing satisfactory results. The trace of a running car is obtained clearly and multiple vehicle tracking is realized in field test. It is believed that Φ-OTDR is promising for vehicle tracking applications.

This work was supported by the National Natural Science Foundation of China (No. 61405227), the National High Technology Research and Development Program of China (No. 2012AA041203), the Science

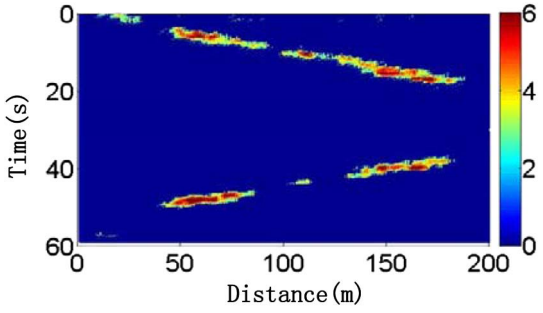

Fig. 7. 2D digital sliding filtering processed waterfall pattern.

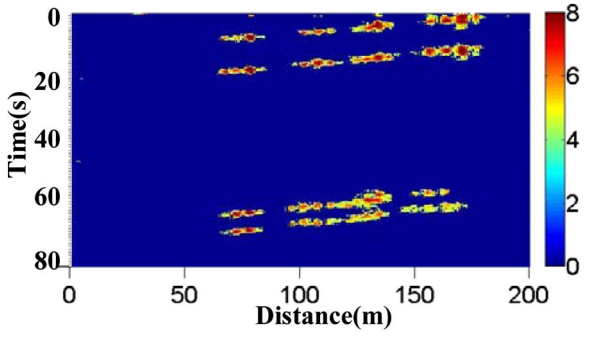

Fig. 8. Waterfall detected for four cars running successively.

and Technology Commission of Shanghai Municipality (Nos. 11DZ1140202 and 13XD1425400).

References

1. N. Ye, Z. Wang, R. Malekian, Y. Zhang, and R. Wang, J. Sensors **2015**, 210298 (2015).
2. Y. Ning, W. Zhong-qin, R. Malekian, W. Ru-chuan, and A. H. Abdullah, Elektronika Ir Elektrotechnika **19**, 105 (2013).
3. K. Finkenzeller, *RFID Handbook: Fundamentals and Applications in Contactless Smart Cards and Identification*, 2nd ed. (John Wiley & Sons, 2002).
4. C. Sungur, H. B. Gökgündüz, and A. A. Altun, in *Proceedings of the 2014 Federated Conference on Computer Science and Information Systems (FedCSIS)* (2014), p. 1353.
5. X. Zhang, F. Zhang, S. Li, M. Wang, L. Wang, Z. Song, Z. Sun, H. Qi, C. Wang, and G. Peng, Chin. Opt. Lett. **12**, S10608 (2013).
6. K. N. Choi, J. C. Juarez, and H. F. Taylor, Proc. SPIE **5090**, 134 (2003).
7. H. F. Martins, S. Martin-Lopez, P. Corredera, P. Salgado, O. Frazão, and M. González-Herráez, Opt. Lett. **38**, 872 (2013).
8. Z. Pan, Z. Wang, Q. Ye, H. Cai, R. Qu, and Z. Fang, Proc. SPIE **9157**, 91576X (2014).
9. J. Zhou, Z. Pan, Q. Ye, H. Cai, R. Qu, and Z. Fang, J. Lightwave Technol. **31**, 2947 (2013).
10. N. Duan, F. Peng, Y.-J. Rao, J. Du, and Y. Lin, Proc. SPIE **9157**, 91577A (2014).
11. Z. Pan, K. Liang, Q. Ye, H. Cai, R. Qu, and Z. Fang, Proc. SPIE **8311**, 83110S (2011).
12. W. Diao, X. Zhang, J. Liu, X. Zhu, Y. Liu, D. Bi, and W. Chen, Chin. Opt. Lett. **12**, 072801 (2014).
13. R. C. Gonzalez and R. E. Woods, *Digital Image Processing*, 3rd ed. (Publishing House of Electronics Industry, 2010).